Zeeman-level lifetimes in $Er^{3+}:Y_2SiO_5$

S. R. Hastings-Simon,[1] B. Lauritzen,[1] M. U. Staudt,[1] J. L. M. van Mechelen,[2] C. Simon,[1] H. de Riedmatten,[1] M. Afzelius,[1] and N. Gisin[1]

[1]*Group of Applied Physics, University of Geneva, CH-1211 Geneva 4, Switzerland*

[2]*Department of Condensed Matter Physics, University of Geneva, CH-1211 Geneva 4, Switzerland*

(Received 14 April 2008; revised manuscript received 10 July 2008; published 11 August 2008)

We present measurements of Zeeman-level population lifetimes in $Er^{3+}:Y_2SiO_5$ at low magnetic fields and low temperatures. Using spectral hole burning spectroscopy, we investigate the dynamics and temperature dependence of the hole structure due to the Zeeman interaction. Evidence for population storage in Zeeman levels with lifetimes of up to 130 ms is found in the form of long-lived spectral holes and antiholes. We also observe that a subset of the erbium ions exhibit very long-lived holes with lifetimes as long as 60 s at 2.8 K.

DOI: 10.1103/PhysRevB.78.085410 PACS number(s): 78.90.+t, 78.47.−p, 61.72.−y, 32.60.+i

I. INTRODUCTION

Because of their narrow homogenous linewidths and corresponding long optical coherence times at low temperatures, rare-earth (RE)-doped crystals have been the subject of much investigation for photon-echo-based optical data storage and data processing.[1,2] Recently, there has been additional interest in RE-doped crystals, spurred by proposals to extend their use to applications in the fast developing field of quantum communication and computation. In particular, RE-doped crystals are promising materials for the realization of reversible transfer of quantum states between photons and atoms. Such a quantum memory represents a basic building block for the so-called quantum repeater,[3–5] which would allow the extension of quantum communications schemes such as quantum cryptography[6] to much longer distances than with direct transmission.

Several techniques have been proposed for photonic quantum storage, including, electromagnetically induced transparency (EIT),[7–10] off-resonant interactions,[11,12] and photon echoes with controlled reversible inhomogeneous broadening (CRIB).[13–17] An essential building block for quantum memories is a so-called Λ system which couples two ground states via an excited state. Also, for spectral tailoring applications such as isolating a single absorption line within a broad inhomogeneous absorption profile, a Λ system is necessary to have a place to put the absorbers. Λ systems in hyperfine levels have been observed and studied in a variety of RE ions, including praseodymium,[18–20] europium,[21,22] and thulium.[23,24] Another prospective Λ system in RE systems is the ground-state Zeeman levels. Population storage in Zeeman levels in $Nd^{3+}:LaF_3$ at low magnetic field has been investigated,[25] recent work has been done in $Nd^{3+}:YVO_4$,[26] and a footnote[27] has been given for Er^{3+} but to our knowledge there has been no systematic study of a Λ system in Er.

The 1.5 μm, $^4I_{15/2} \rightarrow {}^4I_{13/2}$, transition in Er^{3+} is well matched to standard telecommunication fiber and makes a memory based on Er^{3+} attractive as it would allow simple interfacing of such a memory in a fiber communication network. A memory that stores photons at the telecommunication wavelength is necessary for some quantum repeater protocols.[4,28,29] Moreover this transition is easily accessible with stable diode lasers. In addition, recent investigations show that optical coherence times on the scale of microseconds can be obtained in Er^{3+}-doped silicate fibers[30,31] and on the order of milliseconds in Er^{3+}-doped Y_2SiO_5 crystals.[27] Extensive studies of the spectroscopy and optical coherence properties of Er^{3+}-doped Y_2SiO_5 crystals have been performed.[27,32] The excellent optical coherence times in this material can be attributed to the low nuclear moments of the constituent elements of the host crystal Y_2SiO_5. We here extend previous studies on this material to Zeeman-level population lifetimes, which are relevant for different quantum memory protocols.

Zeeman-level population lifetimes in rare-earth ions at low magnetic fields have in general not been characterized. Measurements in Er-doped Y_2SiO_5 have been performed at high magnetic field using electron paramagnetic resonance (EPR) spectroscopy, where lifetimes of up to 40 ms were found.[33] At high field, spin-lattice relaxation is the dominant process for relaxation and these lifetimes are limited by direct phonon processes which should be greatly reduced at lower fields.[33–35] We resent measurements for $Er^{3+}:Y_2SiO_5$ at low magnetic fields and low temperatures.

Using spectral hole burning (SHB) spectroscopy,[36] we investigate spectral holes in the 1.5 μm, $^4I_{15/2} \rightarrow {}^4I_{13/2}$, transition in $Er^{3+}:Y_2SiO_5$. We observe long-lived spectral holes, which is evidence of a multilevel, long lifetime, and optically accessible structure in the material. We make detailed measurements of the time evolution of the spectral holes and antiholes in the system, allowing us to extract the Zeeman population lifetimes and to estimate the relative transition probabilities within the Zeeman structure.

II. THEORY

A Λ system for quantum memory proposals is one in which two close to degenerate ground-state levels are independently optically coupled to a single excited-state level. Such a system allows transitions between the two ground-state levels via the excited-state level and storage of ions in one of the two ground-state levels. Evidence for optical pumping and a Λ system can be found with SHB measurements. In a two-level system (one ground state and one excited state) an intense laser at a fixed frequency is used to

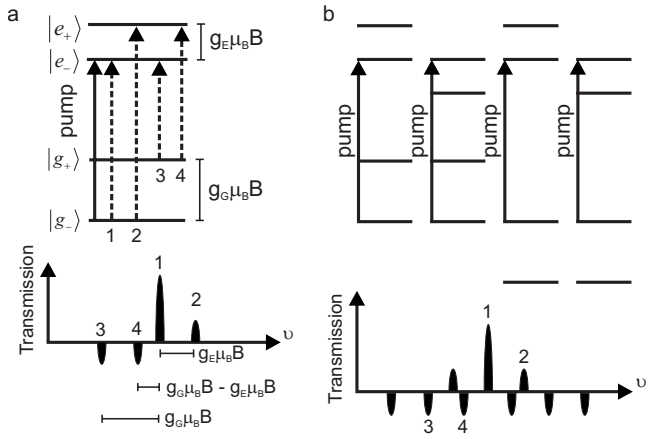

FIG. 1. (a) Four-level hole burning spectrum (Zeeman levels) for the class of ions where the laser is in resonance with the $|g_-\rangle \rightarrow |e_-\rangle$ transition. The g_G (g_E) is the g factor for the ground (excited) state, μ_B is the Bohr magneton, and B is the applied magnetic field. The pump transition (solid line) and possible probe transitions (dashed lines) between the four levels are shown in the energy diagram and labeled on the corresponding transmission spectrum of holes and antiholes. (b) Four level hole burning spectrum with inhomogeneous broadening. The four different classes of ions within the inhomogeneous profile that are in resonance with the pump beam are shown, along with the resulting transmission spectrum of holes and antiholes (here the probe transitions are not shown for clarity).

excite ions from the ground state to an upper excited state. The ions can then be probed by reducing the intensity and scanning the frequency of the laser around the pump frequency. The ions in the excited state lead to a hole in the absorption which is seen as a peak in transmission. In the case of an ion with two ground states and two excited states, for instance, corresponding to Zeeman levels, the spectrum is more complex as the burning frequency can be in resonance with transitions from either of the two ground states to either of the two excited states. These four alternatives correspond to four different classes of ions within the inhomogeneous profile [see Fig. 1(b)]. Ions can be optically pumped via the excited state into the other ground state, leading to an increase in absorption from this other ground state (an antihole). Thus in addition to the central hole one expects additional holes as well as antiholes at spacings given by the Zeeman-level spacings. Figure 1(a) shows the hole burning spectrum for one class of ions; the complete spectrum for the four classes is shown in Fig. 1(b).

In order to have efficient optical pumping and trapping in the second ground-state level, it is necessary to have a relaxation time between the ground-state levels (T_Z) that is much longer than the optical T_1 lifetime of the excited-state transition. In addition one must consider the branching ratio β, which we here define as the probability to return to the initial spin state upon relaxation from the optically excited state. The effective optical T_1 lifetime for the transfer is really the product of the lifetime and the number of cycles needed to change state on relaxation. For spin states this could be much longer than T_1 as the branching ratio β may be close to unity. In the case where T_Z is shorter or of the same order as the effective T_1, ions pumped into the other ground-state level will relax back into the first level. The signature of storage in the ground-state Zeeman levels is the appearance of antiholes at the ground-state Zeeman splitting and a central hole which decays with a lifetime longer than the excited-state T_1 lifetime.

In SHB experiments one measures the transmitted intensity after the crystal of length L. The transmitted intensity at position L, $I(L)$, is given by

$$I(L) = I(0)e^{-\alpha L}, \tag{1}$$

where $I(0)$ is the incident intensity and α is the absorption coefficient. The absorption coefficient at a frequency ω is linearly proportional to the population difference, $N_1 - N_2$, where N_1 (N_2) is the number of ions in the ground (excited) state at ω. Therefore SHB measurements can be used to extract information about the dynamics of the populations. All SHB spectra presented in this paper are the natural logarithm of the measured transmitted intensity. The area of spectral holes and antiholes is also measured from the natural logarithm of the transmitted intensity.

III. EXPERIMENTAL SETUP

The Y_2SiO_5 crystal belongs to the space group C_{2h}^6, and Er^{3+} substitutes for Y^{3+} in two crystallographically inequivalent sites with C_1 symmetry. The substitution of Er^{3+} ions into the two sites appears to be about equal. The erbium $^4I_{15/2}$ ground state is split into eight Kramers doublets, where only the lowest one is populated at liquid-helium temperatures, and the $^4I_{13/2}$ splits into seven doublets. In both cases each Kramers doublets splits into two Zeeman levels with an applied magnetic field. In addition the isotope ^{167}Er has a nonzero nuclear spin which gives rise to a hyperfine interaction. The ^{167}Er isotope is naturally occurring at ~23% percent; the corresponding hyperfine levels have not been studied here.

The Y_2SiO_5 crystal has three mutually perpendicular optical-extinction axes labeled D_1, D_2, and b. The direction of propagation here is always along the b axis. The $Er^{3+}:Y_2SiO_5$ crystal used here is $3\times3.5\times4$ mm^3 along the b, D_1, and D_2 axes, respectively, doped with 10 ppm Er. The magnetic field is applied in the D_1-D_2 plane in order to make the two magnetically inequivalent sites degenerate. This greatly simplifies the complexity of the hole spectrum due to the Zeeman-level structure. Following the convention of Ref. 37 (see Fig. 2), the angle between the magnetic field and the crystal axis is defined with respect to the D_1 axis (i.e., an angle of 0° corresponds to a B field along the D_1 axis and an angle of 90° anticlockwise corresponds to a B field along the D_2 axis). In this work we performed measurements in two directions in the plane D_1-D_2: 90° (parallel to D_2) and 135°.

In our investigation of persistent spectral holes in Er^{3+}-doped Y_2SiO_5 we used a monochromatic laser to excite Er^{3+} ions from the $^4I_{15/2}$ ground state to the $^4I_{13/2}$ excited state, thereby creating a spectral hole at the frequency of the laser. The excitation pulse, or burning pulse, was followed by a sequence of read pulses. These pulses were made by attenuating the laser and scanning the frequency by acting on

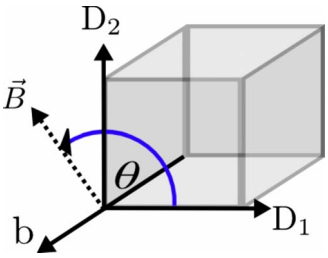

FIG. 2. (Color online) Visualization of the angle of the magnetic field $\vec{B}$ with respect to the axes. $\vec{B}$ lies in the plane spanned by D_1 and D_2. The light propagates in a direction parallel with the b axis.

the laser current. The transmitted light was measured with a photodiode (NewFocus, model 2011). The pulses were made by gating a cw external cavity diode laser (Toptica) using an acousto-optic modulator (AOM). The laser was operated in free running mode and its linewidth within the relevant time range was $\Delta\nu \geq 1$ MHz. The pulse sequence was controlled by an arbitrary function generator. The following results are for a burning laser at 1535.7 nm which corresponds to site 1 (Ref. 27) in the $^4I_{15/2}$ ground state to the $^4I_{13/2}$ excited-state transition. The crystal was cooled to temperatures down to 2 K with a liquid-helium cold finger cryostat (Janis ST400). A temperature sensor was placed on the crystal holder.

IV. RESULTS AND DISCUSSION

A. Hole burning spectra

A typical hole burning spectrum (burning pulse of 200 ms and data averaged over 10 scans) with a waiting time of 1 ms between the burning pulse and readout pulse is shown in Fig. 3(a) for temperatures from 2.05 to 4.6 K with an applied magnetic field of 1.2 mT at 135° in the D_1-D_2 plane. The large central hole is at the frequency of the burning laser. The side antihole (which becomes a hole at higher temperatures) corresponds to population in another level. To confirm that the pattern of holes and antihole measured is due to the Zeeman levels we measured the position of the first side antihole as a function of applied magnetic field. The side hole was

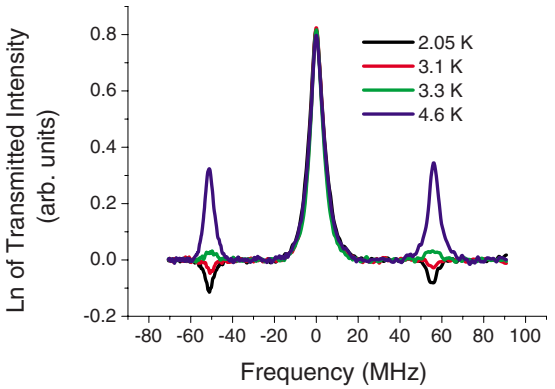

FIG. 3. (Color online) Spectral hole burning spectra recorded 1 ms after the hole burning pulse. Antiholes at first Zeeman splitting become holes for higher temperatures. The magnetic field is 1.2 mT applied at 135° to the D_1 axis in the D_1-D_2 plane.

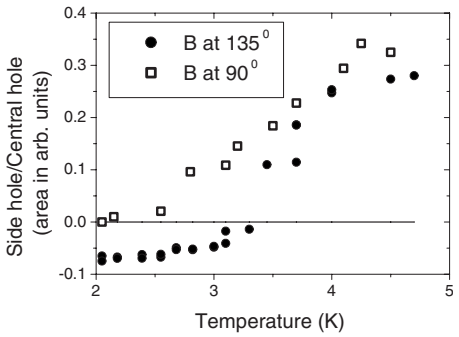

FIG. 4. Ratio of area of antihole to the central hole at 1 ms after burn pulse as a function of temperature for B at 135° (circles), as in Fig. 3, and B at 90° (squares). The line at zero indicates the crossing between hole and antihole.

found to move with the applied field as 50 MHz/mT for a B field at 90°, corresponding to a g factor of 3.6, which is the difference between the ground and excited-state g factors (g_g and g_e, respectively) given in published results[38] for this direction of magnetic field. This antihole corresponds to transition 4 indicated in Fig. 1(a).

The strong hole at the g_g-g_e Zeeman splitting for higher temperatures indicates that the Zeeman lifetime is much shorter than the excited-state lifetime for these temperatures, and thus the pump laser is pumping both ground-state Zeeman levels since they couple strongly. The appearance of antihole at the g_g-g_e Zeeman splitting for lower temperatures indicates that we reach the regime where the Zeeman-level lifetime becomes longer and trapping in the ground-state level begins.

We can examine the crossing into this regime by looking at the size of the central and side holes as a function of temperature. When the side hole becomes an antihole we have significant trapping. This measurement for both B field orientations in the D_1-D_2 plane is shown in Fig. 4. For B at 90° we see that we never cross this critical point; we do not observe significant trapping in the Zeeman levels. However for B at 135° in the D_1-D_2 plane, at temperatures below 3.4 K, the hole becomes an antihole, indicating population trapping. While we see evidence of trapping the ratio of antihole to hole stays small and does not increase significantly with decreasing temperature from 3 to 2 K.

This behavior can be understood qualitatively by the high-magnetic-field spin-relaxation measurements in Er^{3+}-doped Y_2SiO_5 reported by Kurkin and Chernov.[33] Their results can be well reproduced with a standard spin-lattice relaxation (SLR) model.[34,35] Phonons cause relaxation between spin states through direct, Raman, and Orbach processes giving a total SLR rate of

$$\frac{1}{T_1^{\mathrm{SLR}}} = aB^4T + bT^9 + ce^{-\Delta/T}, \tag{2}$$

where B is the magnetic field and T is the temperature and a, b, and c are the scaling factors in the regime where kT is much less than the Zeeman splitting. The magnetic-field-independent Raman and Orbach processes dominate the spin-lattice relaxation rates at a temperature of 4.6 K. From

their measurements we can calculate this rate to be about 3.8 kHz at 4.6 K, corresponding to a T_Z of 0.26 ms, which is much shorter than the optical T_1 of 11 ms.[27] For the measurement of Kurkin and Chernov,[33] the Raman and Orbach processes are strongly suppressed at temperatures below about 3 K and the direct process dominates as relaxation mechanism.[33] The qualitative agreement with the results presented in Fig. 3 is rather good. However, any quantitative comparison between our measurements and those by Kurkin and Chernov[33] below 3 K is difficult because of the strong magnetic-field dependence of the direct process. The two measurements were indeed performed in very different magnetic-field regimes: the experiment of Kurkin and Chernov[33] was performed at high magnetic field (corresponding to a Zeeman splitting of 9 GHz) while our measurement are performed at very small magnetic field (1 mT, corresponding to 100 MHz Zeeman splitting). We will come back to this point in Sec. IV B, where we study the Zeeman relaxation lifetime as a function of temperature.

B. Hole and antihole dynamics

In order to quantitatively measure the Zeeman population lifetimes, we can look at the dynamics of the hole and antihole as a function of time after the burning pulse. We perform these measurements for B oriented at 90° and 135° for temperatures ranging from 2.1 to 3.1 K. The results for B at 135° and the lowest temperature (2.1 K) are discussed here. We measured the fast dynamics of the central hole and side antihole in the first 600 ms following the burning pulse; the decay curves of the central and side holes are shown in Fig. 5(a). These data are also presented as the ratio of the area of the antihole to hole in Fig. 5(b).

The Zeeman-level lifetime can be extracted from an exponential fit of the hole or antihole. For the hole we expect two decays, the first due to the excited-state lifetime of 11 ms (Ref. 27) and the second due to the Zeeman-level lifetime. In order to extract the Zeeman lifetime here we fix the first decay of the spectral hole in our fit at 11 ms and fit simultaneously the hole and antihole slow decays. We find for 2.1 K a lifetime of 129 ± 4 ms; the fit is shown as a solid line. We also find an offset here of roughly 3% which we will discuss later.

The ratio of the antihole to hole, as seen in Fig. 5(b), has two distinct time scales. During the first tens of milliseconds the antihole grows in size as population relaxes from the excited state into the ground-state Zeeman levels. This decreases the size of the hole as there is no longer a contribution from population stored in the excited state. After this period the ratio remains fixed, and both the hole and antihole decay with a common time constant. This further supports the interpretation that population in the Zeeman levels is responsible for the long-lived central hole.

If all the ions were transferred from one Zeeman ground state to the other there would be no population left in the excited state. Hence the hole decay should be a single exponential with a decay time equal to the Zeeman-level lifetime. Instead we observe a double exponential decay with a large component at the 11 ms lifetime indicating that the percentage of ions transferred is small. With the measured lifetime of 129 ms and an excited-state lifetime of 11 ms we would expect a higher percentage of transfer than is observed (see Fig. 6). One likely explanation for this discrepancy is an unequal branching ratio: the probability for an ion to decay

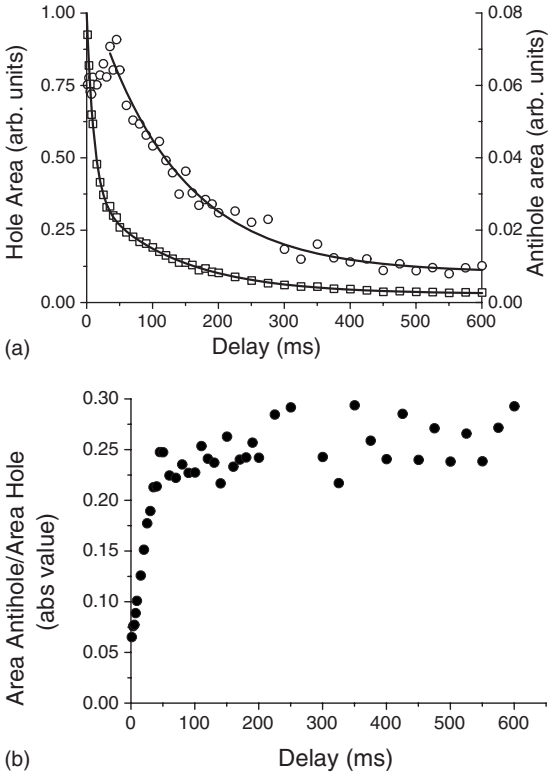

FIG. 5. (a) Area of the antihole (circles, right axis) and hole (squares, left axis) as a function of delay for B at 135°. The solid lines are exponential fits with an extracted Zeeman lifetime of 129 ± 4 ms. The fit for the antihole starts at 50 ms. (b) Ratio of area (absolute value) of antihole to hole as a function of delay for B at 135° in the D_1-D_2 plane. The temperature for this measurement is 2.1 K.

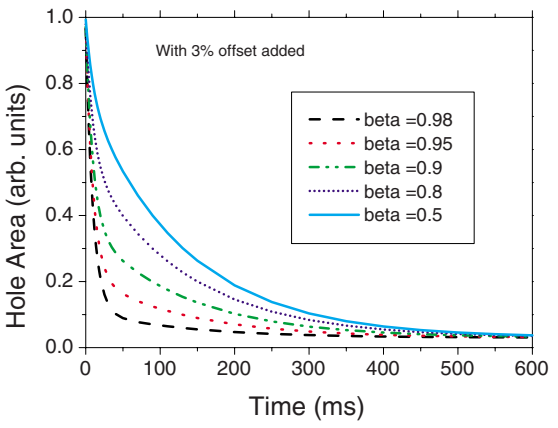

FIG. 6. (Color online) Simulation of hole area as a function of time for optical pumping with different branching ratios β. We assume a Zeeman lifetime of 129 ms for both excited and ground states and an equal β for pumping and relaxation for the various transitions.

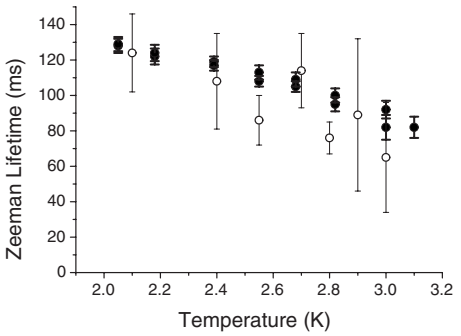

FIG. 7. Zeeman lifetime as a function of temperature for B at 135° (filled circles) and B at 90° (open circles).

from the excited state back into its initial state is large; i.e., it favorably does not change spin. For a transfer from one to the other Zeeman ground-state level, however, an ion has to undergo a change of spin. Therefore many excitation cycles are required for an efficient transfer.

We have constructed a full numerical model for spectral hole burning in a four-level inhomogeneously broadened system (see Appendix). By solving the rate equations in MATLAB we can produce simulations for holes and antiholes as a function of the various lifetimes, pumping rates, and branching ratios. A number of simplifying assumptions are made, most importantly that the Zeeman-level lifetimes are equal for the ground state and excited state (129 ms as measured for the ground state), and that β is the same for absorption and emission. In reality, an appreciable amount of ions will relax through other crystal-field levels in the ground state,[27] which can modify the branching ratio for the emission. In addition we assume that the pump power is high enough to saturate the pump transitions for all four types of ions (see Fig. 1). A plot of the hole area as a function of delay for four different values of β (0.98, 0.95, 0.9, 0.8, and 0.5) is shown in Fig. 6.

If we compare the experimental curve in Fig. 5(a) to these simulations we see the form matches that of a β of 0.9 or higher. Because of the many simplifying assumptions one must be cautious in using the simulations to extract a value for β, but we do find an agreement with the assumption that the β is close to unity in this case. It then follows that β is also an important limiting factor for the percentage of ions transferred between Zeeman levels by the optical pumping.

The Zeeman lifetimes, measured in the same way as above, for both magnetic-field orientations are shown in Fig. 7. The measurements for B at 90° have a larger uncertainty due to the smaller signal-to-noise ratio for the central hole, which is smaller in this case for long delays due to less trapping in the Zeeman levels. However we note the interesting result that the Zeeman-level lifetimes for both angles are similar. This would indicate that the absence of antiholes in the B at 90° case (see Fig. 4) is due to an even worse branching ratio than for B at 135°; in other words that the transition preserves very strongly the spin.

Let us now come back to the comparison between our measurements and those reported by Kurkin and Chernov.[33] We observe that the measured lifetimes measured in this work are shorter than those predicted by an extrapolation from the measured values of 40 ms at high magnetic fields and the B^4 dependence.[33] Similar discrepancies between the expected Zeeman lifetime due to SLR, at low magnetic fields and low temperatures, and the actual measured lifetime have been reported for other ions.[25,26] In general the interactions that drive spin relaxations at low magnetic fields have not been well studied. It appears that other mechanisms than SLR drive the relaxation, possibly spin-spin flip flops between the rare-earth ions or interactions with other magnetic impurities or defect centers.

C. Long-lived holes

We also observed a remaining 3–10% offset in most of our hole decay measurements (independent of the angle of the applied field). The large variation comes from the sensitivity of the offset to the zero delay time which defines the initial amplitude. To investigate this offset in more detail, we study the spectral hole burning spectra after a time much longer than the Zeeman relaxation lifetime for different temperatures. Spectra recorded after a delay of 500 ms following a burning pulse of 800 ms with a magnetic field $B=0.34$ mT applied at 135° are shown in Fig. 8(a) for temperatures between 2.5 and 4.5 K. Similar results can be found for B fields applied at 90°. There is a central hole and two strong antiholes at about 15 MHz from the central hole. These curves are normalized with respect to the maximum transmission for each temperature. Although the amplitude of the hole/antihole structure is decaying with temperature, we note that the ratio between antihole and hole remains roughly constant. The additional weak antiholes close to the central hole we believe to be due to superhyperfine interaction, presumably with yttrium ions. Population trapping in superhyperfine levels has been observed previously.[25]

We also measured the dynamics of the central hole over many tens of seconds. The measurement sequence was 30 s of a burning pulse followed by low-intensity "readout pulses" every 1.5 s for 40 s with a magnetic field of 0.58 mT applied at 90°. To ensure that light leakage during the waiting periods as well as the readout pulse did not reburn a hole we measured the spectral hole signal with no burning pulse after a long waiting time and found no hole. The central hole decay could be fitted using a single exponential function, where the decay constant is the hole lifetime. We measured the hole lifetime for different temperatures in the range of 1.5–4.5 K and found a clear dependence of the lifetime on the temperature [see Fig. 8(b)]. In addition we verified that the lifetime of the adjacent antihole matched that of the central hole, suggesting that the origin of the long-lived hole can be explained by the existence of the adjacent antihole which traps the population.

To determine the character of the long-lived hole we measured the splitting of the antihole from the central hole as a function of applied field and found that it varies as around 50 MHz/mT, as also found for the antihole at shorter delays. Moreover, we observe no hole or antihole without a magnetic field [see Fig. 8(a)]. This would indicate that the long-lived hole has a magnetic Zeeman character as well. We measured the lifetimes of the central hole here to be 60 s at

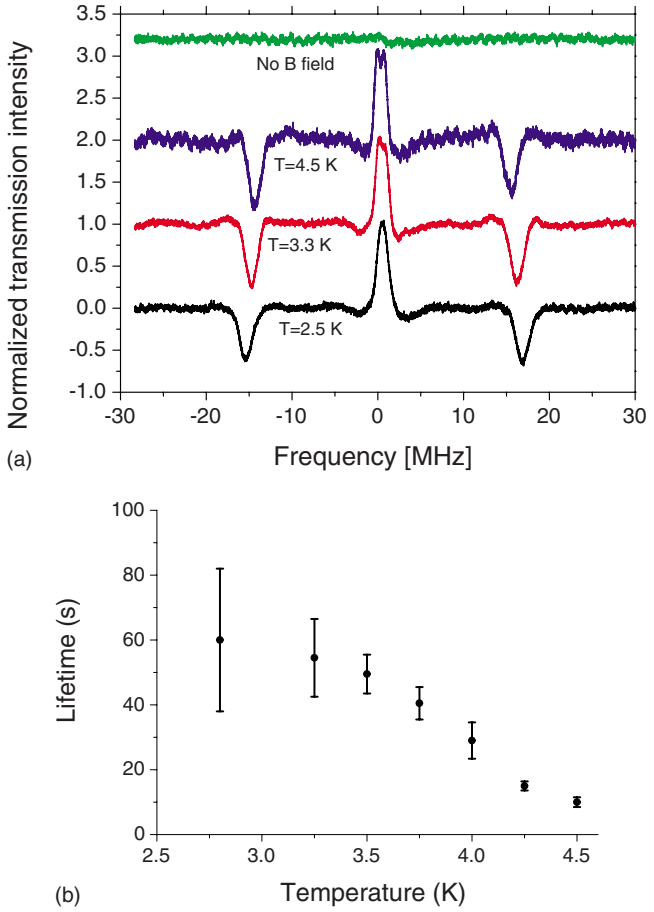

FIG. 8. (Color online) (a) Spectral hole burning spectrum after 500 ms for $B=0.34$ mT at 135° for temperatures from 2.5 to 4.5 K. The spectra are normalized with respect to the maximal transmission for each temperature and shifted vertically for clarity. (b) Lifetimes of the long-lived central hole for $B=0.58$ mT at 90° as a function of temperature.

2.8 K. This is much longer than one would expect for Zeeman levels at this temperature based on previous spin-lattice relaxation measurements.[33] However it is particularly the weak temperature dependence of the spectra recorded at long delays [Fig. 8(a)], as compared to the short delay spectra (Fig. 3), which is surprising. While the temperature dependence at short delays could be understood qualitatively using the results of Kurkin and Chernov,[33] as discussed above, the temperature dependence at long delays is puzzling. It appears that this 3–10% subset of ions does not couple as efficiently to phonons, although we have not found a satisfying reason for this behavior.

We believe it is possible that such long-lived holes exist in other similar systems. Because the lifetime is so long compared with the other time scales of interest, this hole appears as simply an offset for measurements up to many hundreds of milliseconds.

V. CONCLUSIONS

We have experimentally investigated the Zeeman-level population trapping in $Er^{3+}:Y_2SiO_5$ at low magnetic fields and low temperatures. We have measured Zeeman state lifetimes of up to 129 ± 4 ms and shown evidence that the branching ratio is not well adapted for optical pumping. If this branching ratio can be improved, however, this system is a good candidate for realization of efficient optical pumping. For instance, one could imagine us to use rf excitation in the excited state to increase the branching ratio via mixing of population between spin states. Also, one could induce stimulated emission to a ground-state level to decrease the effective excited-state lifetime, which would further improve the transfer of population between Zeeman states. In addition to these results, we have also observed very long lifetime holes (60 s) for a subset of 3–10% of the ions. The mechanism for this slow relaxation is not clear and further measurements are necessary to clarify these results.

ACKNOWLEDGMENTS

We would like to thank the group of D. van der Marel for their hospitality during the measurements and L. Bonacina and M. Chergui (EPFL) for the use of the liquid-helium cryostat. We also thank O. Guillot-Noël and P. Goldner for stimulating discussions. Technical support by M. Brandt, C. Barreiro, and J. D. Gautier is acknowledged. This work was supported by the Swiss NCCR Quantum Photonics and the European Commission under the Integrated Project Qubit Applications (QAP) funded by the IST directorate as Contract No. 015848.

APPENDIX: SIMULATION OF OPTICAL PUMPING IN A FOUR-LEVEL SYSTEM WITH INHOMOGENEOUS BROADENING

This appendix presents the model used for the simulations of Fig. 6. We consider a four-level system with two ground states (level 1 and 2) and two excited states (level 3 and 4). We also include the inhomomogeneous broadening of the optical transitions. The interaction with the pump laser is modeled through standard rate equations, which include optical absorption, emission, and stimulation terms, as well as spin-relaxation terms. The system of rate equations describing evolution of the fractional populations ρ_1, ρ_2, ρ_3, and ρ_4 can be written as

$$\frac{d\rho_1}{dt} = -(w_{12}+R_{13}+R_{14})\rho_1 + w_{21}\rho_2 + (A_{31}+R_{13})\rho_3 + (A_{41}+R_{14})\rho_4, \tag{A1}$$

$$\frac{d\rho_2}{dt} = w_{12}\rho_1 - (w_{21}+R_{23}+R_{24})\rho_2 + (A_{32}+R_{23})\rho_3 + (A_{42}+R_{24})\rho_4, \tag{A2}$$

$$\frac{d\rho_3}{dt} = R_{13}\rho_1 + R_{23}\rho_2 + w_{43}\rho_4 - (A_{31}+A_{32}+w_{34} + R_{13}+R_{23})\rho_3, \tag{A3}$$

$$\frac{d\rho_4}{dt} = R_{14}\rho_1 + R_{24}\rho_2 + w_{34}\rho_3 - (A_{41} + A_{42} + w_{43} + R_{14} + R_{24})\rho_4, \quad \text{(A4)}$$

where w_{ij} are the spin-relaxation rates, A_{ij} are the Einstein coefficients, and R_{ij} are the pumping rates for the transition $i \rightarrow j$. The Einstein coefficients and pump rates are related through the same branching coefficient, for instance, $\beta = A_{31}/(A_{31}+A_{32}) = R_{13}/(R_{13}+R_{23})$. The ground-state spin lifetime T_Z that is experimentally measured in this work is related to the spin-relaxation rates as

$$1/T_Z = w_{12} + w_{21}. \quad \text{(A5)}$$

When the thermal energy is larger than the spin state splitting, as is the case in our work, then $w_{12}=w_{21}$ and $w_{34}=w_{43}$. Moreover, the pumping rates are given by

$$R_{ij} = \frac{2\pi^2}{3n\epsilon_0 ch^2}|\mu_{ij}|^2 I(\nu) g(\nu - \nu_{ij}), \quad \text{(A6)}$$

where μ_{ij} is the dipole moment, $I(\nu)$ is the intensity of the pump laser, and $g(\nu-\nu_{ij})$ is a Lorentzian function describing the homogeneously broadened line with resonance frequency ν_{ij}.

The model treats the inhomogeneous broadening as a discrete set of classes of ions with their resonance frequencies ν_{ij} shifted by the detuning $\Delta\nu$. For each class of ions the set of rate equations are integrated for the duration of the hole burning pulse using a monochromatic pump laser. This results in a set of population factors ρ_1, ρ_2, ρ_3, and ρ_4 as a function of detuning $\Delta\nu$ due to the interaction with the burn pulse. To calculate the evolution of population between the burn and scan pulse, all pump terms R_{ij} are set to zero and the rate equations are further integrated in time to simulate the spectral hole decay. Using the population factors calculated at different times, we can reconstruct a complete inhomogeneous hole burning spectrum and its time evolution.

[1] M. Mitsunaga, Opt. Quantum Electron. **24**, 1137 (1992).
[2] S. Kröll and U. Elman, Opt. Lett. **18**, 1834 (1993).
[3] H.-J. Briegel, W. Dür, J. I. Cirac, and P. Zoller, Phys. Rev. Lett. **81**, 5932 (1998).
[4] L.-M. Duan, M. D. Lukin, J. I. Cirac, and P. Zoller, Nature (London) **414**, 413 (2001).
[5] C. Simon, H. de Riedmatten, M. Afzelius, N. Sangouard, H. Zbinden, and N. Gisin, Phys. Rev. Lett. **98**, 190503 (2007).
[6] N. Gisin, G. Ribordy, W. Tittel, and H. Zbinden, Rev. Mod. Phys. **74**, 145 (2002).
[7] M. Fleischhauer and M. D. Lukin, Phys. Rev. Lett. **84**, 5094 (2000).
[8] T. Chanelière, D. N. Matsukevich, S. D. Jenkins, S. Y. Lan, T. A. B. Kennedy, and A. Kuzmich, Nature (London) **438**, 833 (2005).
[9] M. D. Eisaman, A. André, F. Massou, M. Fleischhauer, A. S. Zibrov, and M. D. Lukin, Nature (London) **438**, 837 (2005).
[10] J. J. Longdell, E. Fraval, M. J. Sellars, and N. B. Manson, Phys. Rev. Lett. **95**, 063601 (2005).
[11] B. Julsgaard, J. Sherson, J. I. Cirac, J. Fiurasek, and E. S. Polzik, Nature (London) **432**, 482 (2004).
[12] J. Nunn, I. A. Walmsley, M. G. Raymer, K. Surmacz, F. C. Waldermann, Z. Wang, and D. Jaksch, Phys. Rev. A **75**, 011401(R) (2007).
[13] S. A. Moiseev and S. Kröll, Phys. Rev. Lett. **87**, 173601 (2001).
[14] M. Nilsson and S. Kröll, Opt. Commun. **247**, 393 (2005).
[15] B. Kraus, W. Tittel, N. Gisin, M. Nilsson, S. Kröll, and J. I. Cirac, Phys. Rev. A **73**, 020302(R) (2006).
[16] A. L. Alexander, J. J. Longdell, M. J. Sellars, and N. B. Manson, Phys. Rev. Lett. **96**, 043602 (2006).
[17] G. Hétet, J. J. Longdell, A. L. Alexander, P. K. Lam, and M. J. Sellars, Phys. Rev. Lett. **100**, 023601 (2008).
[18] K. Holliday, M. Croci, E. Vauthey, and U. P. Wild, Phys. Rev. B **47**, 14741 (1993).
[19] M. Nilsson, L. Rippe, S. Kröll, R. Klieber, and D. Suter, Phys. Rev. B **70**, 214116 (2004).
[20] E. Fraval, M. J. Sellars, and J. J. Longdell, Phys. Rev. Lett. **95**, 030506 (2005).
[21] W. R. Babbitt, A. Lezama, and T. W. Mossberg, Phys. Rev. B **39**, 1987 (1989).
[22] M. Nilsson, L. Rippe, N. Ohlsson, T. Christiansson, and S. Kröll, Phys. Scr. **T102**, 178 (2002).
[23] N. Ohlsson, M. Nilsson, S. Kröll, and R. K. Mohan, Opt. Lett. **28**, 450 (2003).
[24] F. de Sèze, A. Louchet, V. Crozatier, I. Lorgere, F. Bretenaker, J. L. Le Gouët, O. Guillot-Noël, and P. Goldner, Phys. Rev. B **73**, 085112 (2006).
[25] R. M. Macfarlane and J. C. Vial, Phys. Rev. B **36**, 3511 (1987).
[26] S. R. Hastings-Simon, M. Afzelius, J. Minář, M. U. Staudt, B. Lauritzen, H. de Riedmatten, N. Gisin, A. Amari, A. Walther, S. Kröll, E. Cavalli, and M. Bettinelli, Phys. Rev. B **77**, 125111 (2008).
[27] T. Böttger, C. W. Thiel, Y. Sun, and R. L. Cone, Phys. Rev. B **74**, 075107 (2006).
[28] N. Sangouard, C. Simon, J. Minář, H. Zbinden, H. de Riedmatten, and N. Gisin, Phys. Rev. A **76**, 050301(R) (2007).
[29] N. Sangouard, C. Simon, B. Zhao, Y.-A. Chen, H. de Riedmatten, J.-W. Pan, and N. Gisin, Phys. Rev. A **77**, 062301 (2008).
[30] R. M. Macfarlane, Y. Sun, P. B. Sellin, and R. L. Cone, Phys. Rev. Lett. **96**, 033602 (2006).
[31] M. U. Staudt, S. R. Hastings-Simon, M. Afzelius, D. Jaccard, W. Tittel, and N. Gisin, Opt. Commun. **266**, 720 (2006).
[32] T. Böttger, C. W. Thiel, Y. Sun, and R. L. Cone, Phys. Rev. B **73**, 075101 (2006).
[33] I. Kurkin and K. Chernov, Physica B & C **101**, 233 (1980).
[34] D. A. Davids and P. E. Wagner, Phys. Rev. Lett. **12**, 141 (1964).
[35] G. H. Larson and C. D. Jeffries, Phys. Rev. **141**, 461 (1966).
[36] R. Macfarlane and R. Shelby, in *Spectroscopy of Crystals Containing Rare Earth Ions*, edited by A. Kaplyankii and R. Macfarlane (Elsevier Science, Amsterdam, The Netherlands, 1987).
[37] Y. Sun, T. Böttger, C. W. Thiel, and R. L. Cone, Phys. Rev. B **77**, 085124 (2008).
[38] T. Böttger, Ph.D. thesis, Montana State University, 2002.